New Journal of Physics
The open-access journal for physics

Secular variation of the Earth's magnetic field: induced by the ocean flow?

Gregory Ryskin
Robert R McCormick School of Engineering and Applied Science, Northwestern University, Evanston, IL 60208, USA
E-mail: ryskin@northwestern.edu

New Journal of Physics **11** (2009) 063015 (23pp)
Received 12 March 2009
Published 12 June 2009
Online at http://www.njp.org/
doi:10.1088/1367-2630/11/6/063015

Abstract. Secular variation of the Earth's main magnetic field is believed to originate in the Earth's core. (The main field is operationally defined as comprising spherical harmonics of degree $l \leqslant 10$.) I propose a different mechanism of secular variation: ocean water being a conductor of electricity, the magnetic field induced by the ocean as it flows through the Earth's main field may depend on time and manifest itself globally as secular variation. This proposal is supported by calculation of secular variation using the induction equation of magnetohydrodynamics, the observed main field and the ocean flow field. The predicted secular variation is in rough agreement with that observed. Additional support is provided by the striking temporal correlation (hitherto unsuspected) between the intensity of the North Atlantic oceanic circulation and the rate of secular variation in Western Europe; this explains, in particular, the geomagnetic jerks, and the recently discovered correlation between secular variation and climate. Spatial correlation between ocean currents and secular variation is also strong.

Contents

1. Introduction

The Earth's magnetic field is varying on timescales from milliseconds to millions of years. Of particular interest is secular variation of the geomagnetic main field (Langel 1987), on timescales of years to centuries and beyond. (The main field is operationally defined as comprising spherical harmonics of degree $l \leqslant 10$.) Owing to secular variation, the International Geomagnetic Reference Field (IGRF) must be revised every 5 years (IGRF 2007). Since secular variation is believed to originate in the Earth's core (this notion can be traced to the proposal by Edmond Halley (1692)), theoretical studies of secular variation have been limited to solving the inverse problem: find the flow at the core–mantle boundary that would produce the observed secular variation (Bloxham *et al* 1989, Hulot *et al* 2002, Olsen and Mandea 2008, Olson and Aurnou 1999). The results of these studies cannot be compared with observations: seismic data indicate that the Earth's outer core is fluid, but flow in the core cannot be measured or observed.

I propose a different mechanism of secular variation: ocean water being a conductor of electricity, the magnetic field induced by the ocean as it flows through the Earth's main field may depend on time and manifest itself globally as secular variation.

This proposal can be divided into three parts as follows:

(a) The ocean-induced magnetic field certainly exists, and may depend on time, including, possibly, on annual and longer timescales. If the spherical harmonic expansion of its year-to-year variation contains low-degree terms, these cannot be separated from secular variation of the main field, just as the low-degree spherical harmonics of the crustal field (if they exist) cannot be separated from the steady main field.

(b) The crucial question is whether the ocean-induced field may vary on secular variation timescales. The bulk of the present work (sections 2–7) deals with this issue. Fortunately, one is on a firm ground here: the analysis is based on magnetohydrodynamics. The difficulties, though considerable, are largely mathematical; no hypotheses need to be invoked or introduced. The answer is in the affirmative, and the spherical harmonic

expansion of the ocean-induced secular variation can be calculated, the low-degree terms in particular.

(c) Given (a) and (b), the only remaining question is whether the ocean-induced secular variation is a part or the whole of the observed secular variation. In principle, this question should be easy to answer by comparing the results of calculations in (b) with the observational data, but in practice such a comparison is complicated by the incompleteness of data, the manner of data representation, the limited precision of the computations, etc. In addition, a possibility of significant error in the numerical results cannot be excluded. Thus, while the comparison in section 7 does suggest that secular variation in its entirety is induced by the ocean flow, this by no means constitutes a proof of the proposal. In fact, a definitive proof may never be possible, but as the accuracy and completeness of the data continue to improve, and further computations are carried out, sufficient clarity on this issue should be achieved soon.

This paper is organized in a somewhat unusual way: after a brief statement of governing equations, a lengthy interlude follows where a simpler model problem is discussed in detail; this is followed by the detailed statement of the present problem, the description of mathematical approach, and the discussion of results. Analysis of observational data is also included, to further support the conclusions. The interlude was deemed necessary because in the present case the standard approach—state the equations and boundary conditions, and then seek an appropriate mathematical method—is doomed to failure: the problem becomes intractable already at the statement stage. Only having a good grasp of the expected result makes it possible to suggest a mathematical formulation of the problem that allows solution at reasonable cost.

2. The governing equations

Due to its salt content, ocean water has substantial electrical conductivity, $\sigma \approx 3.2\,\mathrm{S\,m^{-1}}$. Weak electric currents are induced in seawater as it moves through the Earth's magnetic field; these currents give rise to secondary magnetic fields, which add to the original field. Evolution of the total field is described by the induction equation of magnetohydrodynamics (Moffatt 1978),

$$\frac{\partial \mathbf{B}}{\partial t} = \nabla \times (\mathbf{u} \times \mathbf{B}) + \eta \nabla^2 \mathbf{B}. \tag{1}$$

Here $\mathbf{B}(\mathbf{r}, t)$ is the magnetic field (flux density), $\mathbf{u}(\mathbf{r}, t)$ is the velocity of the fluid, and $\eta \equiv (\mu_0 \sigma)^{-1}$ is the magnetic diffusivity (μ_0 is a constant of SI). Since no magnetic charges exist, $\mathbf{B}(\mathbf{r}, t)$ is solenoidal,

$$\nabla \cdot \mathbf{B} = 0. \tag{2}$$

A formal statement of the problem would include conditions at the boundaries with neighboring domains, and also governing equations and boundary conditions in all those domains (the Earth's crust, mantle, core, etc). Stated in this way, the problem becomes intractable. On the other hand, limiting the domain of solution to the ocean, and imposing the observed main field as boundary conditions, eliminates any chance of finding what causes secular variation. The formulation presented below circumvents these difficulties by exploiting the great disparity, in the ocean case, of the characteristic timescales of the field advection and diffusion.

Magnetic diffusion in the ocean is extremely fast, essentially instantaneous on the secular variation timescales. The magnetic diffusivity of seawater is $\eta \approx 0.25\,\mathrm{km^2\,s^{-1}}$; the characteristic time of diffusion through the depth of the ocean, $(\mathrm{depth})^2/\eta$, is $\sim$1 min. The global ocean diffusion timescale is longer but still very short compared with the secular variation timescales: for the ocean viewed as a thin spherical shell of constant thickness H and radius R (the Earth's radius), this timescale is $RH/\eta \sim 1$ day (Callarotti and Schmidt 1983).

This means that magnetic field in the ocean always satisfies $\nabla^2\mathbf{B} = 0$ to a very good approximation. The effect of advection in this case is subtle, and leads to surprising results. The mathematical formulation of the problem presented below is far from straightforward; to motivate it, let us first consider a simpler model problem.

3. A model problem: advection and diffusion of solute in slow flow

In a flow of a dilute solution, evolution of the solute concentration $c(\mathbf{r}, t)$ is described by the advection–diffusion equation

$$\frac{\partial c}{\partial t} = -\mathbf{u}\cdot\nabla c + D\nabla^2 c, \tag{3}$$

where D is the molecular diffusion coefficient. Consider a class of problems such that the characteristic timescale of diffusion is much shorter than the timescales of both advection and the temporal variation in boundary conditions. Then $c(\mathbf{r}, t)$ always satisfies $\nabla^2 c = 0$ to a very good approximation. This does not preclude $c(\mathbf{r}, t)$ from changing with time (slowly).

For example, if the boundary conditions are time-dependent, $c(\mathbf{r}, t)$ will vary with time even though it satisfies the steady equation $\nabla^2 c = 0$ (the quasi-steady-state approximation, akin to the adiabatic approximation in quantum mechanics). This is a common situation, analogous to the time-dependent flow with negligible inertia forces in fluid dynamics (Batchelor 1967). Note that in this case $c(\mathbf{r}, t)$ is not influenced by advection at all.

Another, admittedly rare, situation may also arise: $c(\mathbf{r}, t)$ may vary with time not because its variation is imposed by the boundary conditions, but due to the effect of advection—if the advection-caused variation in $c(\mathbf{r}, t)$ is such that $c(\mathbf{r}, t)$ continues to satisfy $\nabla^2 c = 0$ at all times. (While the boundary conditions are not causing this variation, they need to be sufficiently 'soft' to allow it.) An example is found in the Taylor dispersion phenomenon.

Taylor (1953) analyzed what happens when a molecular dye is introduced into a liquid flowing slowly through a tube (Poiseuille flow). For example, the dye may initially fill uniformly a given cross-section, so that its concentration as a function of the axial coordinate x represents a pulse. (Concentration is presumed to be independent of the angular coordinate, $c = c(x, r, t)$.) If diffusion were absent, the dye would be advected by the flow, forming a continuously lengthening paraboloid. For a slow flow in a long, thin capillary, diffusion in the axial direction (along the streamlines) can indeed be neglected, but diffusion in the radial direction cannot. Equation (3) then becomes

$$\frac{\partial c}{\partial t} = -u\frac{\partial c}{\partial x} + \frac{D}{r}\frac{\partial}{\partial r}\left(r\frac{\partial c}{\partial r}\right) \equiv T(c), \tag{4}$$

where $u = u(r)$ is the velocity of the Poiseuille flow. $T(c)$, where T is a linear operator, denotes the right-hand side of the equation.

Taylor considered the case when the timescale of diffusion in the radial direction is very short compared with the advection timescale. Concentration within each cross-section is then kept nearly uniform by diffusion at all times. Taylor predicted that the 'patch of colour' (the solute concentration profile) should move (translate) with the mean speed of flow U. He pointed out that this conclusion is 'most remarkable... since water moves at twice the mean speed near the centre of the pipe and the patch of colour at the mean speed, the clear water in the middle must approach the colour patch, absorb colour as it passes into it and then lose colour as it passes out, finally leaving the patch as perfectly clear water'. Taylor ended his analysis with these words: 'This theoretical conclusion seemed so remarkable that I decided to set up apparatus to find out whether the predictions of the analysis could be verified experimentally'. The experiment fully confirmed his predictions.

In modern language (Gorban and Karlin 2005), Taylor exploited the great disparity of the characteristic timescales of diffusion and advection, and sought a solution within the *slow manifold* (a function subspace) to which the system is driven, on the fast timescale, by diffusion. The slow manifold is then the subspace $\mathcal{G}$ whose elements are functions of x (and t), independent of r. (The elements of the original function space of solutions are functions of x, r and t.) Consider a linear operator P_G whose action is averaging over a cross-section, i.e. for any $f(x, r, t)$,

$$P_G(f) = \frac{2}{a^2}\int_0^a f r \, \mathrm{d}r, \tag{5}$$

where integration is from 0 at the axis to the internal radius of the tube a. Clearly, P_G is a projection on $\mathcal{G}$: P_G satisfies the operator equation $P_G^2 = P_G$, and acts as identity operator within $\mathcal{G}$ (Halmos 1957). P_G is defined uniquely by the requirement that its action must mimic the effect of diffusion in the radial direction when advection is absent or negligible.

To describe the evolution of concentration profile within the slow manifold $\mathcal{G}$, the operator T in equation (4) is projected on $\mathcal{G}$, the result being formally $P_G T P_G$ (Gorban and Karlin 2005). The elements of $\mathcal{G}$ do not depend on r; accordingly, upon projection the advection operator $-u\partial/\partial x$ loses its dependence on r and becomes $-U\partial/\partial x$, whereas the diffusion operator disappears altogether ($\mathcal{G}$ is a subspace of the null space of the radial diffusion operator). Thus, the slow-manifold evolution equation for the cross-sectional-average concentration $P_G(c) \equiv \hat{c}(x, t)$ is

$$\frac{\partial \hat{c}}{\partial t} = -U\frac{\partial \hat{c}}{\partial x}. \tag{6}$$

The seemingly paradoxical disappearance of the dominant term is the hallmark of the projection-on-the-slow-manifold approach (Gorban and Karlin 2005); the effect of the dominant term (here, the uniformity of concentration within cross-section) is enforced by the projection. Note that the original two-dimensional problem, with dependence on x and r, has been reduced to a one-dimensional one, with dependence on x only.

The general solution of equation (6) is an arbitrary function of x translating along x with velocity U, exactly as Taylor (1953) predicted. Note that the dependence of solution on time is fully determined by advection projected on the slow manifold; the molecular diffusivity D must be large to justify the projection, but its magnitude does not influence the result.

Thus, considering advection and diffusion of solute under somewhat restrictive conditions that nevertheless encompass a large class of problems, Taylor made a conclusion of great generality. His next step was to calculate the correction to the above solution, arising from

the fact that D is large but not infinite. Using equation (4) in the frame of reference moving with velocity U (where the above solution becomes a steady profile), Taylor calculated the small (inversely proportional to D) deviation of concentration from uniformity within a cross-section, $\delta(x, r)$, and the advective flux of solute across the cross-section due to $\delta(x, r)$. That led to his second general conclusion: because of this flux, the translating concentration profile must slowly spread out in the axial direction in a diffusion-like manner, the effective coefficient of this 'dispersion' being inversely proportional to the molecular diffusivity D. (This 'Taylor dispersion' effect is now used to measure molecular diffusivities.) Note that the same advection–diffusion equation, under two different assumptions, was used to analyze two different aspects of the same phenomenon. Only the first of these aspects, the diffusion-modified advection, has a direct analogue in the present problem. The dispersion effect will not concern us further.

To summarize, temporal evolution of a physical system described by an advection–diffusion equation such as equation (3), with diffusion being the dominant effect, may occur via two completely different mechanisms: (i) imposed externally through variation of boundary conditions, or (ii) caused internally by the diffusion-modified advection.

Suppose now that we observe evolution of such a physical system, but the boundary conditions are unknown; how can we ascertain which mechanism of the two is at work? The answer is simple: calculate the effect of the diffusion-modified (projected on the slow manifold) advection, and compare with observations. If they agree, there can be little doubt that advection is the cause of the evolution. It could be argued that variation of the unknown boundary conditions could also cause the system to evolve in exactly the same way as the advection calculations predict; such an explanation would not survive Occam's razor, however.

Let us now return to the ocean flow and the geomagnetic field.

4. Formulation of the problem in physical terms

As discussed above, magnetic field in the ocean $\mathbf{B}(\mathbf{r}, t)$ always satisfies $\nabla^2\mathbf{B} = 0$ to a very good approximation. This also applies everywhere in the thin spherical shell at the Earth's surface that contains the ocean (the domain of solution to be described below) because the magnetic diffusivity of the rock is even greater than that of the seawater. Moreover, in the same limit of $\eta \to \infty$ or $\sigma \to 0$, the current $\mathbf{J}$ vanishes. Since $\nabla \times \mathbf{B} = \mu_0\mathbf{J}$, magnetic field in the ocean is, to a very good approximation, irrotational, and can be expressed as a gradient of a scalar function, $\mathbf{B} = -\nabla\psi$. Together with $\nabla \cdot \mathbf{B} = 0$, this guarantees that $\nabla^2\mathbf{B} = 0$. In addition, the magnetic scalar potential $\psi(\mathbf{r}, t)$ satisfies $\nabla^2\psi = 0$. With a slight abuse of terminology, such solenoidal irrotational vector fields will be called 'harmonic' below.

A distortion by the ocean flow that makes the magnetic field non-harmonic is immediately eliminated—reduced to a very small magnitude—by diffusion. (Since η is large but not infinite, a small non-harmonic contribution $\mathbf{b}(\mathbf{r})$ to the total field survives, analogous to $\delta(x, r)$ in Taylor's problem.) Diffusion is, however, indifferent to such flow-produced changes in the field that do not violate harmonicity, i.e. such that the field potential remains a sum of solid spherical harmonics (solutions of Laplace's equation), but the coefficients of the harmonics become functions of time. I propose that such flow-induced changes constitute secular variation; if so, the latter can be calculated as $\partial\mathbf{B}/\partial t$ given by equation (1). The calculation is far from straightforward: as in Taylor's case, it requires projection on the slow manifold to which the system is driven, on the fast timescale, by magnetic diffusion.

In the existing studies of the ocean-induced magnetic field, secular variation is neglected and $\partial\mathbf{B}/\partial t$ in equation (1) is set to zero. (For a complete formulation of the problem considered in the existing studies, see Stephenson and Bryan (1992). Recent work is reviewed by Kuvshinov (2008).) Setting $\partial\mathbf{B}/\partial t$ in equation (1) to zero eliminates the possibility of seeing the time-dependent effects of steady advection, considered in the present work. Instead, the non-harmonic contribution $\mathbf{b}(\mathbf{r})$ is found from equation (1) in the form

$$0 = \nabla\times(\mathbf{u}\times\mathbf{B}) + \eta\nabla^2\mathbf{b}, \tag{7}$$

where the observed main field is used for $\mathbf{B}$. The resulting field $\mathbf{b}(\mathbf{r})$ is of the order of a few nanotesla in magnitude (Manoj *et al* 2006, Stephenson and Bryan 1992, Vivier *et al* 2004). For a steady ocean flow $\mathbf{u}(\mathbf{r})$, the field $\mathbf{b}(\mathbf{r})$ has no time dependence, and can hardly be observed: the crustal field is typically much greater. If the ocean flow used in equation (7) is time-dependent, $\mathbf{b}$ may inherit its temporal variability: with $\mathbf{u}(\mathbf{r},t)$ varying on tidal or longer timescales, equation (7) describes a valid quasi-steady-state approximation (Tyler *et al* 2003, Vivier *et al* 2004). Whether time-dependent or not, $\mathbf{b}$ cannot be compared, or related in any other way, to $\partial\mathbf{B}/\partial t$ calculated below—these are two different aspects of the same phenomenon. ($\mathbf{b}(\mathbf{r})$ is analogous to $\delta(x, r)$ in Taylor's problem.) Not only $\mathbf{b}$ and $\partial\mathbf{B}/\partial t$ have different dimensions, but $\mathbf{b}$ also depends (inversely) on η, whereas $\partial\mathbf{B}/\partial t$ does not.

In the present calculations, the ocean flow is steady (averaged over a five-year interval), equation (1) is used in its full time-dependent form, and only the geomagnetic main field and its secular variation are of interest; consequently, $\mathbf{B}$ and $\partial\mathbf{B}/\partial t$ are required to be harmonic vector fields. This restriction—enforced by projection on the harmonic subspace—entails no loss of rigor when only the slow dynamics of the main field is sought. It leaves undetermined the non-harmonic part of the induced field—the subject of the previous studies—and the induced currents manifest themselves only globally, via slow (secular) variation of the main field.

The harmonic subspace is spanned by vector fields whose scalar potentials are solid spherical harmonics; projection on the harmonic subspace—which plays the role of slow manifold—filters out the fast diffusional modes, in the same way as setting to zero $\partial\mathbf{E}/\partial t$ in the Maxwell equations filters out electromagnetic waves (Moffatt 1978).

The slow-manifold evolution found in the present work is closely analogous to Taylor's (1953) first result: in a flow through a capillary tube, the solute concentration profile is translating with the mean velocity of the flow because diffusion keeps the concentration nearly uniform within cross-section. The second result of Taylor (1953)—the dispersion in the axial direction due to the small deviation from uniformity $\delta(x, r)$—has no observable analogue in the present problem: dispersion of the advected field by a similar mechanism is negligible compared with the extremely fast magnetic diffusion, which acts in all spatial directions (see equation (4) of Young and Jones (1991)). If this dispersion were observable, the two aspects of the phenomenon, $\partial\mathbf{B}/\partial t$ calculated in the present work and $\mathbf{b}$ considered in the existing literature, could be used together to evaluate it, along the lines of Taylor (1953).

5. Formulation of the problem in mathematical terms

Direct numerical simulation is not feasible in this problem due to the widely separated timescales of advection and diffusion (the problem is computationally 'stiff'). The present approach is, essentially, operator splitting: the preliminary—not necessarily harmonic—version

of $\partial\mathbf{B}/\partial t$ is found from equation (1) with the diffusion term omitted; this version is then projected on the subspace of harmonic fields, thus enforcing the effect of diffusion. (Actually, the projection is done in two steps: one performed before the advection calculation, and one after.) This approach is akin to Chorin's (1969) projection method, where the preliminary—not necessarily solenoidal—version of the velocity field is computed from the Navier–Stokes equation with the pressure gradient omitted; it is then projected on the subspace of solenoidal vector fields, thus enforcing the effect of the pressure gradient. In Chorin's case, the subspace of solenoidal vector fields plays the role of slow manifold, to which the system is driven, on the fast timescale, by the pressure gradient (pressure change propagates with the speed of sound). The incompressible fluid approximation, which filters out the sound waves from the equations of fluid dynamics, is precisely the requirement that the velocity field belong to this slow manifold, defined by $\nabla \cdot \mathbf{u} = 0$.

Unknown boundary conditions present an even greater difficulty than computational stiffness. The projection method described below has a crucial advantage: it eliminates the need for boundary conditions by reducing the problem to a two-dimensional one, on the Earth's surface. This is analogous to Taylor's (1953) reduction of a two-dimensional problem to a one-dimensional one.

With a prescribed velocity field $\mathbf{u}$, the right-hand side of the induction equation (1)

$$\frac{\partial \mathbf{B}}{\partial t} = \nabla \times (\mathbf{u} \times \mathbf{B}) + \eta \nabla^2 \mathbf{B}$$

is a linear operator acting on $\mathbf{B}(\mathbf{r}, t)$, viz.,

$$\frac{\partial \mathbf{B}}{\partial t} = A(\mathbf{B}) + \eta \nabla^2 \mathbf{B}, \tag{8}$$

where A is the advection operator, defined by

$$A(\mathbf{B}) \equiv \nabla \times (\mathbf{u} \times \mathbf{B}). \tag{9}$$

To describe the evolution within the slow manifold—the harmonic subspace—the operator $A + \eta\nabla^2$ of equation (8) is projected on this subspace (Gorban and Karlin 2005). The main field is defined as comprising solid spherical harmonics of degree $l \leqslant N$; consequently, only harmonics of degree $l \leqslant N$ must be included in the subspace. (In the IGRF main-field models, $N = 10$ until the year 2000, and 13 thereafter.) Let us denote this subspace by $\mathcal{M}$, and the operator of projection on $\mathcal{M}$ by P_M. It follows immediately that the operator ∇^2 projected on $\mathcal{M}$, i.e. $P_M \nabla^2 P_M$, is a zero operator ($\mathcal{M}$ is a subspace of the null space of ∇^2). Thus, the slow-manifold evolution equation for $\mathbf{B}(\mathbf{r}, t)$ is

$$\frac{\partial \mathbf{B}}{\partial t} = P_M A\, P_M(\mathbf{B}), \tag{10}$$

where $P_M A\, P_M$ is the advection operator A projected on $\mathcal{M}$.

Note the crucial difference between equation (10) and the equation

$$\frac{\partial \mathbf{B}}{\partial t} = A(\mathbf{B}), \tag{11}$$

which describes advection of a field by a highly conducting fluid: whereas equation (11) follows from equation (1) by neglecting the diffusion term in the limit $\eta \to 0$, in equation (10) the projection P_M guarantees that the evolving field $\mathbf{B}(\mathbf{r}, t)$ remains harmonic and so always satisfies the equation $\nabla^2\mathbf{B} = 0$, which describes the opposite limit $\eta \to \infty$. That is, although the diffusion term is not explicitly present in equation (10), its effect is fully enforced by the projection.

In order to calculate $\partial\mathbf{B}/\partial t$ using equation (10), the operator A projected on $\mathcal{M}$ must be expressed by means of explicit mathematical operations. Let us first recall some examples of projections. We have encountered one particularly simple projection in the discussion of Taylor's problem. Another common type of projection is a truncated expansion of a given function in elements of a complete orthogonal set that forms a basis in the function space. Such a truncated expansion (e.g. a truncated Fourier series of a function defined on a unit circle, or a truncated expansion in surface spherical harmonics of a function defined on a unit sphere, etc) is a projection on the subspace spanned by the selected functions of the set. The orthogonality of the set then leads to the familiar formulae for the expansion coefficients.

Projecting on the subspace $\mathcal{M}$ is a different matter: solid spherical harmonics—solutions of Laplace's equation in three dimensions—do not form a complete basis set in the space of functions $f(\mathbf{r})$ defined in the three-dimensional physical space (and reasonably well-behaved). Let the physical space be described by the spherical coordinates r, θ, ϕ, where r is the distance from the center of the Earth ($r = R$ at the Earth's surface), θ is the colatitude ($\theta = 0$ at the North Pole) and ϕ is the longitude. Then the solid spherical harmonics that span the subspace $\mathcal{M}$ can be written in the following form (in terms of scalar potentials):

$$\left(\frac{R}{r}\right)^{l+1} Y_l^m(\theta, \phi), \qquad 1 \leqslant l \leqslant N, \quad |m| \leqslant l, \tag{12}$$

where $Y_l^m(\theta, \phi)$ is the surface spherical harmonic of degree l and order m, a properly normalized product of an associated Legendre function $P_l^m(\cos\theta)$ and $e^{im\phi}$. (In geomagnetism, Schmidt's normalization is used, known as Racah's normalization in quantum mechanics.) By construction of $\mathcal{M}$, the harmonics in (12) are those used in the representation of the main-field scalar potential

$$\psi = R\sum_{l=1}^{N}\left(\frac{R}{r}\right)^{l+1}\sum_{m=0}^{l}[g_l^m\cos m\phi + h_l^m \sin m\phi]P_l^m(\cos\theta), \tag{13}$$

where g_l^m and h_l^m are Gauss coefficients (IGRF 2007, Langel 1987). Strictly speaking, the ocean-induced field may also include harmonics of the form $(r/R)^l Y_l^m(\theta, \phi)$. These, however, cannot be present in the field observed above the Earth's surface, for $r \geqslant R$, because the field must tend to zero at infinity; also, the thin-shell approximation introduced below would lump together the two solid harmonics with the same $Y_l^m(\theta, \phi)$. The subspace $\mathcal{M}$ defined by (12) is thus adequate for present purposes.

A general procedure of projecting on solid spherical harmonics will not be necessary here; a greatly simplified procedure will suffice, as described below. But first let us consider the advection operator A in greater detail. Since $\nabla\cdot\mathbf{B} = 0$, and $\nabla\cdot\mathbf{u} = 0$ for an incompressible fluid, the advection operator A defined in equation (9) can be written as

$$A(\mathbf{B}) = -\mathbf{u}\cdot\nabla\mathbf{B} + \mathbf{B}\cdot\nabla\mathbf{u}. \tag{14}$$

In the present work, the domain of solution is the thin spherical shell of constant thickness H which includes the ocean; H is $\sim 10^{-3}$ of the Earth's radius $R = 6371$ km. Within this shell, the gradient operator in equation (14),

$$\nabla \equiv \mathbf{e}_r \frac{\partial}{\partial r} + \frac{\mathbf{e}_\theta}{r} \frac{\partial}{\partial \theta} + \frac{\mathbf{e}_\phi}{r \sin\theta} \frac{\partial}{\partial \phi}, \tag{15}$$

can be replaced to a very good approximation by $\mathbf{e}_r \partial/\partial r + \nabla_h$, where ∇_h is the two-dimensional (horizontal) gradient operator on the Earth's surface

$$\nabla_h \equiv \frac{\mathbf{e}_\theta}{R} \frac{\partial}{\partial \theta} + \frac{\mathbf{e}_\phi}{R \sin\theta} \frac{\partial}{\partial \phi}. \tag{16}$$

Let us write $\mathbf{u} = u_r \mathbf{e}_r + \mathbf{u}_h$, where u_r is the vertical velocity and $\mathbf{u}_h \equiv u_\theta \mathbf{e}_\theta + u_\phi \mathbf{e}_\phi$ is the horizontal one. (The coordinate-system conventions differ in oceanography and geomagnetism, so the *u, v, w* notation will not be used here.) A similar decomposition can be written for other vector fields, such as **B**, etc. Then

$$\mathbf{u} \cdot \nabla \mathbf{B} = \left(u_r \frac{\partial}{\partial r} + \mathbf{u}_h \cdot \nabla_h \right) \mathbf{B}. \tag{17}$$

For the fields **B** that belong to the subspace $\mathcal{M}$, derivatives in all spatial directions are of the same order of magnitude (the minimum half-wavelength $\pi R/N \sim 2 \times 10^3$ km), but the velocity components that multiply these derivatives differ greatly in their orders of magnitude. The velocities in equation (17) are those of the time-average large-scale ocean flow. The horizontal velocities are typically ~ 1 to $10\,\mathrm{cm\,s^{-1}}$, reaching $\sim 1\,\mathrm{m\,s^{-1}}$ in western boundary currents. The vertical velocities, on the other hand, are extremely small, and impossible to measure directly; a reasonable estimate is $10^{-6}\,\mathrm{m\,s^{-1}}$ (Pedlosky 1996). Therefore, the vertical velocity u_r will be neglected in what follows. (This issue may be worth revisiting if reliable vertical-velocity data become available.) The operator A in equation (10) now becomes

$$A(\mathbf{B}) = -\mathbf{u}_h \cdot \nabla_h \mathbf{B} + \mathbf{B} \cdot \nabla \mathbf{u}_h. \tag{18}$$

Note that **B** is not differentiated with respect to r. This suggests a simple way to implement the projection on $\mathcal{M}$ required in equation (10), as follows.

The domain of solution is the thin spherical shell of radius R and thickness H, where $H/R \sim 10^{-3}$; using the local vertical coordinate z with $z = 0$ at the Earth's surface, this shell is described by $-H \leqslant z \leqslant 0$. Since $N \cong 10$, within this shell the solid spherical harmonics that span the subspace $\mathcal{M}$ vary in the radial direction by no more than $\sim 1\%$. Thus, within the domain and the precision of the present computation, the elements of $\mathcal{M}$ can be viewed as independent of z. (This reflects the fact that magnetic diffusion within the ocean keeps **B** nearly independent of z at all times.) Projection on a subspace whose elements are independent of z is accomplished by averaging over z, the result being a function of θ, ϕ (and time). This is analogous to projection on the subspace $\mathcal{G}$ in Taylor's problem, where the solute concentration within each cross-section was kept nearly uniform by diffusion. But unlike in Taylor's problem, where the elements of $\mathcal{G}$ were arbitrary (differentiable) functions of x, the elements of $\mathcal{M}$ as functions of θ, ϕ are linear combinations of surface spherical harmonics $Y_l^m(\theta, \phi)$ with $l \leqslant N$. Projection of an arbitrary

function of θ, ϕ on this subset of $Y_l^m(\theta, \phi)$ is just a truncated expansion in surface spherical harmonics: the latter form a complete orthogonal basis in the space of functions defined on a sphere.

This means that in equation (10) (but not in its derivation from equation (1)), projection P_M can be replaced to a very good approximation by $P_Y P_S$, where P_S performs averaging over z, i.e.

$$P_S(f) = \frac{1}{H} \int_{-H}^{0} f \, \mathrm{d}z, \tag{19}$$

whereas P_Y performs expansion in surface spherical harmonics up to degree N. It is easy to see that the operators P_S and P_Y commute, and that P_S and P_Y each satisfy the operator equation $P^2 = P$ and so are projections (Halmos 1957). Note that when vectors are added (integrated over z) in the process of averaging, they must be parallel-transported along the z-coordinate line to a single point (with the same coordinates θ and ϕ); it is convenient to choose this point at the Earth's surface, $z = 0$. Thus P_S projects onto the function subspace $\mathcal{S}$ of vector and scalar fields that depend only on two angular coordinates θ and ϕ (and time), and are defined on the two-dimensional physical space of the sphere $r = R$; this physical space (the Earth's surface) will be denoted S_E below.

Let us now reformulate equation (10) in terms of $P_S(\mathbf{B})$. This is a combination of two fields defined on S_E: a horizontal vector field $P_S(\mathbf{B}_h) \equiv \mathbf{B}_{sh}(\theta, \phi, t)$, which transforms as a two-dimensional vector under the change of coordinates θ, ϕ on S_E, and the projection on $\mathcal{S}$ of the radial (vertical) component $P_S(B_r) \equiv B_{sr}(\theta, \phi, t)$, which behaves as a scalar field on S_E (cf Schutz 1980, p 161). This combination of two fields will be denoted $\mathbf{B}_s(\theta, \phi, t)$ where no confusion may arise. In particular, if $\mathbf{B}(r, \theta, \phi, t)$ belongs to the subspace $\mathcal{M}$, then $\mathbf{B}$ is nearly independent of z within the shell $-H \leqslant z \leqslant 0$, so that $\mathbf{B}_{sh}(\theta, \phi, t) = \mathbf{B}_h(R, \theta, \phi, t)$ and $B_{sr}(\theta, \phi, t) = B_r(R, \theta, \phi, t)$.

The slow-manifold evolution of the magnetic field is then described by the two-dimensional equation on the Earth's surface (actually, two equations, for $\mathbf{B}_{sh}$ and B_{sr})

$$\frac{\partial \mathbf{B}_s}{\partial t} = P_Y A_S P_Y(\mathbf{B}_s). \tag{20}$$

Here A_S is the advection operator A of equation (18) projected on the subspace $\mathcal{S}$ of fields defined on S_E. $\mathbf{B}_s$ belongs to $\mathcal{S}$, and the action of A_S is confined to $\mathcal{S}$. That is, A_S is a two-dimensional (horizontal) operator acting on the Earth's surface; an explicit form of A_S will be derived shortly. Physically, this crucial simplification arises because the fast magnetic diffusion within the ocean keeps the field nearly independent of z at all times; as a result, the field lines take part in the fluid motion only to the extent that they can translate without bending or turning. P_S is analogous to P_G in Taylor's problem, which accounted for the fast radial diffusion across the tube. In both cases, the ultimate effect of the projection is to reduce the dimensionality of the problem.

In applications of equation (20), the initial value of $\mathbf{B}_s(\theta, \phi, t)$ is likely to be the observed main field at the Earth's surface (e.g. the IGRF main field at $r = R$). Represented by a spherical harmonic model, such an initial field necessarily belongs to the subspace with projection P_Y, so that at the initial moment $P_Y(\mathbf{B}_s) = \mathbf{B}_s$. The evolution described by equation (20) will then guarantee that $\mathbf{B}_s(\theta, \phi, t)$ will always belong to the subspace with projection P_Y,

so that $P_Y(\mathbf{B}_s) = \mathbf{B}_s$ at all times. Thus, in all such applications, including the present work, equation (20) becomes

$$\frac{\partial \mathbf{B}_s}{\partial t} = P_Y A_S(\mathbf{B}_s), \tag{21}$$

a two-dimensional equation on the Earth's surface. To calculate $\partial\mathbf{B}/\partial t$ from equation (21), two steps are required: first $A_S(\mathbf{B}_s)$ is computed (using, e.g. a finite-difference approximation for A_S), then the result is expanded in surface spherical harmonics up to degree N.

If P_Y were absent, equation (21) would be completely analogous to equation (6) in Taylor's problem. The presence of P_Y in equation (21) reflects the fact that in the present problem diffusion is the dominant effect in all spatial directions. (In Taylor's case, diffusion in the axial direction was neglected.) P_Y accounts for the effect of diffusion in the horizontal plane, i.e. along the Earth's surface. In particular, secular variation is observed over the continents because the movement of the field lines locally, determined by A_S, is accompanied by redistribution of the field globally via the action of P_Y.

Let us now derive the explicit form of A_S. The operator A defined by equation (18) depends on the horizontal velocity field $\mathbf{u}_h$. The latter must be projected on $\mathcal{S}$ because A_S will operate within $\mathcal{S}$. (This removes the dependence of $\mathbf{u}_h$ on z, which could lead to bending or turning of the field lines.) Let us denote the projection of $\mathbf{u}_h$ on $\mathcal{S}$ as follows:

$$P_S(\mathbf{u}_h) \equiv \mathbf{v}(\theta, \phi, t), \tag{22}$$

this is the ocean flow total horizontal transport divided by H. The vector field $\mathbf{v}$ is a two-dimensional (surface) flow on S_E, and transforms as a two-dimensional vector under the change of coordinates θ, ϕ. (Definition (22) is general; in the computations described below $\mathbf{v}$ is independent of time.)

The gradient operator ∇ projected on the subspace $\mathcal{S}$ is the horizontal gradient operator ∇_h defined in equation (16). With $\mathbf{u}_h$ projected according to equation (22), the velocity gradient tensor $\nabla\mathbf{u}_h$ projected on $\mathcal{S}$ becomes $\nabla_h\mathbf{v}$, a two-dimensional tensor on S_E. Equation (18) projected on $\mathcal{S}$ becomes a pair of equations valid on S_E, the Earth's surface, viz.

$$A_S(\mathbf{B}_{sh}) = -\mathbf{v}\cdot\nabla_h\mathbf{B}_{sh} + \mathbf{B}_{sh}\cdot\nabla_h\mathbf{v}, \tag{23}$$

describing the advection (transport and stretching) on S_E of the horizontal field $\mathbf{B}_{sh}$ by the surface flow $\mathbf{v}$, and

$$A_S(B_{sr}) = -\mathbf{v}\cdot\nabla_h B_{sr}, \tag{24}$$

describing the advection by the surface flow of the radial component B_{sr} (which on S_E behaves as a scalar). Note that equations (23) and (24) are true tensor equations in the two-dimensional space S_E; they remain valid under arbitrary coordinate transformations on S_E.

The total horizontal transport is horizontally non-divergent (Pedlosky 1996), so that

$$\nabla_h\cdot\mathbf{v} = 0. \tag{25}$$

Consequently, equation (24) can be put into the form

$$A_S(B_{sr}) = -\nabla_h\cdot(\mathbf{v}B_{sr}). \tag{26}$$

The form (24) is, however, more convenient for numerical computation because the ocean velocity field is not differentiated.

Equation (24) will be used extensively in the computations described below; an alternative derivation of it, directly from equation (14), is therefore of interest. The radial component of equation (14) is, exactly (see Batchelor 1967, appendix 2),

$$[A(\mathbf{B})]_r = -\mathbf{u}\cdot\nabla B_r + \mathbf{B}\cdot\nabla u_r, \tag{27}$$

since the vertical velocity is neglected, this becomes

$$[A(\mathbf{B})]_r = -\mathbf{u}_h\cdot\nabla_h B_r. \tag{28}$$

To proceed to A_S, the operator $\mathbf{u}_h\cdot\nabla_h$ in equation (28) is projected on the subspace $\mathcal{S}$ and applied to the similarly projected B_r; this leads to equation (24).

The original advection operator A and the two-dimensional advection operator A_S acting on S_E are expressed most coherently by means of the Lie derivative formalism. The Lie derivative of a scalar field $f(\mathbf{r})$ along a vector field $\mathbf{q}(\mathbf{r})$ is (see, e.g. Schutz 1980)

$$\pounds_{\mathbf{q}} f = \mathbf{q}\cdot\nabla f, \tag{29}$$

whereas the Lie derivative of a vector field $\mathbf{a}(\mathbf{r})$ along a vector field $\mathbf{q}(\mathbf{r})$ is

$$\pounds_{\mathbf{q}}\mathbf{a} = \mathbf{q}\cdot\nabla\mathbf{a} - \mathbf{a}\cdot\nabla\mathbf{q}. \tag{30}$$

In terms of its action on the field being differentiated ($f(\mathbf{r})$ or $\mathbf{a}(\mathbf{r})$ in the above), the Lie derivative is a linear operator that obeys the product (Leibniz) rule. The Lie derivative is also linear with respect to the vector field (the flow) along which it acts, i.e.

$$\pounds_{\alpha\mathbf{q}+\beta\mathbf{w}} = \alpha\pounds_{\mathbf{q}} + \beta\pounds_{\mathbf{w}} \tag{31}$$

for arbitrary constants α and β and vector fields $\mathbf{q}$ and $\mathbf{w}$.

Equation (14) can be written as

$$A(\mathbf{B}) = -\pounds_{\mathbf{u}}\mathbf{B}, \tag{32}$$

i.e. for an incompressible fluid, the advection operator A is the negative of the Lie derivative along the flow field $\mathbf{u}$,

$$A = -\pounds_{\mathbf{u}}. \tag{33}$$

Equation (11), describing the advection of a frozen-in field (in the absence of diffusion) by an incompressible fluid flow, becomes

$$\frac{\partial\mathbf{B}}{\partial t} = -\pounds_{\mathbf{u}}\mathbf{B}. \tag{34}$$

Generally, the equation

$$\frac{\partial\Gamma}{\partial t} = -\pounds_{\mathbf{u}}\Gamma \tag{35}$$

describes pure advection by an incompressible (non-divergent) fluid flow $\mathbf{u}$ of any non-diffusing (frozen-in) entity whose spatial distribution is given by $\Gamma(\mathbf{r}, t)$, a scalar, vector, or tensor field;

see, e.g. Tur and Yanovsky (1993). If the fluid is compressible, Γ in equation (35) is replaced by Γ/ρ, where ρ is the density of the fluid.

Consider now the two-dimensional advection operator A_S acting on S_E. Equations (23) and (24) can be written as

$$A_S(\mathbf{B}_{sh}) = -\pounds_{\mathbf{v}}\mathbf{B}_{sh}, \tag{36}$$

$$A_S(B_{sr}) = -\pounds_{\mathbf{v}}B_{sr}. \tag{37}$$

That is, the two-dimensional advection operator A_S acting on S_E is the negative of the two-dimensional Lie derivative along the surface flow $\mathbf{v}$,

$$A_S = -\pounds_{\mathbf{v}}. \tag{38}$$

The main results of the present section can be summarized as follows:

1. Projected on the subspace $\mathcal{S}$ of fields defined on the Earth's surface S_E, the geomagnetic main field becomes a combination of the horizontal field $\mathbf{B}_{sh}(\theta, \phi, t)$, which transforms as a two-dimensional vector under the change of coordinates θ, ϕ on S_E, and the radial component $B_{sr}(\theta, \phi, t)$, which behaves as a scalar field on S_E.
2. Projection on $\mathcal{S}$ of the advection operator $A = -\pounds_{\mathbf{u}}$ amounts to replacing the Lie derivative $\pounds_{\mathbf{u}}$ along the ocean flow $\mathbf{u}(\mathbf{r}, t)$ with the Lie derivative $\pounds_{\mathbf{v}}$ along the surface flow $\mathbf{v}(\theta, \phi, t)$, the latter being the projection on $\mathcal{S}$ of $\mathbf{u}(\mathbf{r}, t)$. (This key result is ultimately a consequence of the linearity of Lie derivative with respect to the flow along which it acts, equation (31).)
3. The diffusion-modified advection of the main field by the ocean flow is described by two equations valid on the Earth's surface

$$\frac{\partial \mathbf{B}_{sh}}{\partial t} = P_Y(-\pounds_{\mathbf{v}}\mathbf{B}_{sh}), \tag{39}$$

$$\frac{\partial B_{sr}}{\partial t} = P_Y(-\pounds_{\mathbf{v}}B_{sr}), \tag{40}$$

where P_Y performs expansion in surface spherical harmonics up to degree N. (For the field $\mathbf{B}_{sh}$, vector spherical harmonics must be used, see, e.g. Schutz (1980).)

For comparison with observations, it is sufficient to calculate the radial component of $\partial\mathbf{B}/\partial t$ at the Earth's surface, using equation (40). The spherical harmonic coefficients of the radial component are very simply related to those of the scalar potential (Backus *et al* 1996); the coefficients of $\partial\psi/\partial t$, thus obtained, can be compared with the IGRF secular variation coefficients that represent observations. Calculations involving $\partial\mathbf{B}_{sh}/\partial t$ would be less expedient; also, numerical differentiation of the ocean velocity field, required in equation (39), would be likely to introduce large errors. Therefore in the present work only the radial component of $\partial\mathbf{B}/\partial t$ was computed, using equation (40). All the quantities in equations (39) and (40) are defined on the Earth's surface; to simplify notation, B_{sr} will be written as B_r from now on. The explicit form of equation (40) is

$$\frac{\partial B_r}{\partial t} = P_Y(-\mathbf{v}\cdot\nabla_h B_r), \tag{41}$$

a two-dimensional equation on the Earth's surface. Here $\mathbf{v}$ is the ocean-flow total horizontal transport divided by H, the thickness of the spherical shell that includes the ocean; ∇_h is the horizontal gradient operator; B_r is the radial component of the main field; and P_Y performs expansion in surface spherical harmonics up to degree N.

Equation (41) is a close analogue of equation (6) in Taylor's problem. The physical picture implied by equations (39)–(41) is that the ocean flow drags the magnetic field lines, but very slowly, with much slip, because within the ocean the field must remain nearly independent of depth and the field lines take part in the fluid motion only to the extent that they can translate without bending or turning. (A mechanical analogy is the slow drift of a very long cable, stretched vertically between a surface float and a weight that hovers over the seafloor.) This dragging of the field lines by the ocean flow is felt globally through the action of the operator P_Y, which accounts for magnetic diffusion in the horizontal plane, i.e. along the Earth's surface.

6. Numerical computation

To calculate $\partial B_r/\partial t$ according to equation (41), first the quantity $-\mathbf{v}\cdot\nabla_h B_r$ is computed by finite-differences, then $\partial B_r/\partial t$ is obtained by expanding the result in spherical harmonics up to degree N. Knowing the expansion coefficients of $\partial B_r/\partial t$, those of $\partial\psi/\partial t$ are found easily (Backus *et al* 1996). The spherical harmonic coefficients of $\partial\psi/\partial t$ are the final results of the calculations, to be compared with the IGRF secular variation coefficients which represent observations.

The IGRF secular variation coefficients are the differences between Gauss coefficients of two successive IGRF main-field models, divided by the five-year interval between the models (IGRF 2007). Accordingly, $\partial B_r/\partial t$ for a selected IGRF five-year interval is calculated using on the right-hand side of equation (41) the ocean flow field averaged over that interval, and B_r of the IGRF main field at the beginning of that interval. (Using instead the interpolated main field at the midpoint of the interval does not change the results.) The IGRF five-year interval is thus treated as a single time slice at which $\partial B_r/\partial t$ is calculated. This is done once only; marching forward in time is not necessary for the present application. Consequently, only minimal computing resources are required; the tasks that take most of the time are downloading the ocean flow field, and performing the spherical harmonic expansion.

The IGRF main-field models are available at five-year intervals starting in 1900. For the interval 1995–2000, selected for the present study, a high-quality estimate of the ocean flow field is also available (Köhl *et al* 2007). The quantity $-\mathbf{v}\cdot\nabla_h B_r$ was computed on the $1^\circ\times 1^\circ$ computational grid covering the Earth's surface, using a second-order finite-difference approximation. The values of $B_r(\theta,\phi)$ on the grid were obtained using the IGRF-10 main-field model for 1995 (IGRF 2007). The maximum depth of the ocean (excluding the deep trenches) was read off the hypsometric curve, yielding $H = 6000$ m. The ocean flow field, averaged over the time span January 1995–January 2000, was downloaded from the ECCO-SIO $1^\circ\times 1^\circ$ adjoint dataset for 1992–2002, using a Live Access (LAS) server (ECCO 2007). (On land, $\mathbf{v}$ was set to zero.) Adjoint datasets combine the ocean observation data with a numerical general circulation model, the latter used essentially for smoothing (interpolating) the data (Köhl *et al* 2007, Wunsch and Heimbach 2007). The datasets extend to the depth of 5700 m, but are most reliable in the upper 1000 m, where the observational data are much more numerous, and where

most of the grid points of the numerical model are concentrated. The upper 1000 m is also where more than 90% of the oceanic transport occurs (Curry and McCartney 2001). Therefore only the data for the upper 1000 m were integrated to obtain the horizontal transport vector. To account for the scarcity of the geomagnetic observatories in the Southern Ocean region (see below), the results of the finite-difference predictor at the grid points south of 45°S were ignored when calculating the expansion coefficients of $\partial B_r/\partial t$.

Several checks of the numerical procedure were performed before the actual computation of $\partial B_r/\partial t$. The spherical harmonics part (finding the expansion coefficients of a function specified on the grid, with subsequent transition from the coefficients of the radial component to the coefficients of the scalar potential) was checked by applying it to $B_r(\theta, \phi)$ whose values on the grid were obtained from the IGRF main-field model; this resulted in recovering Gauss coefficients of the latter with excellent accuracy. The finite-difference part was checked separately, using test functions $\mathbf{q}(\theta, \phi)$ and $f(\theta, \phi)$ for which $\mathbf{q} \cdot \nabla_h f$ could be calculated analytically for comparison. The integral of B_r and thus also of $\partial B_r/\partial t$ over the entire Earth's surface must vanish (because $\nabla \cdot \mathbf{B} = 0$); this constraint was well satisfied by the results. In spite of these checks, a possibility of significant error in the numerical results should not be discounted. The complexity of the input data precludes order-of-magnitude estimation of the expected results.

7. Numerical results and comparison with IGRF

The calculated $\partial \mathbf{B}/\partial t$ is expanded in spherical harmonics; table 1 compares the first eight expansion coefficients of its potential $\partial \psi/\partial t$ with the IGRF secular variation coefficients that represent observations (IGRF 2007). Before discussing table 1, a few remarks are in order. The IGRF main-field spherical harmonic coefficients (Gauss coefficients) are found by the least squares fit to the local field data. As is well known to the practitioners of this procedure, it is ill-conditioned: small changes in the data can lead to large changes in the coefficients because different combinations of basis functions may fit the data about equally well (Press *et al* 1992, p 670). In particular, using data from different sets of observatories, or weighting them in different ways, may lead to very different coefficients. Compare, e.g. the global field model with a regional (Continental US) model (Macmillan and Quinn 2000): with the exception of the dominant axial-dipole coefficient g_1^0, the main-field coefficients differ by a large factor and/or sign, whereas the secular variation coefficients bear no resemblance whatsoever. Since the crustal field is not expected to contribute to the low-degree main-field coefficients (Langel 1987), and cannot influence the secular variation coefficients, these differences are entirely due to the differences in the geographical distribution and weighting of the data used in construction of the two models. Thus, if comparison with the IGRF is contemplated, theoretical calculations should strive to mimic the geographical distribution of data used in the IGRF models. This is not easily done: the distribution of the geomagnetic observatories over the globe is highly non-uniform, being especially poor in the Southern Ocean region (Macmillan and Quinn 2000). Only a minimal adjustment could be made in the present calculations to account for this non-uniformity (see above).

In view of the above, the agreement in table 1 between the calculated values of the first four coefficients and their IGRF values is better than could be expected. These coefficients are the most important ones: the first three determine the apparent decrease in the Earth's magnetic moment and the secular motion of the geomagnetic (dipole) poles that define the geomagnetic

Table 1. Secular variation coefficients for the 1995–2000 time span (nT yr^{-1}).

	$\dot{g}_1^0$	$\dot{g}_1^1$	$\dot{h}_1^1$	$\dot{g}_2^0$	$\dot{g}_2^1$	$\dot{h}_2^1$	$\dot{g}_2^2$	$\dot{h}_2^2$
This work	15.0	8.7	−20.6	−14.3	7.1	17.4	−9.3	−16.7
IGRF	14.5	11.2	−24.0	−13.5	−0.3	−23.1	−2.0	−9.0

coordinate system (used in solar-terrestrial and magnetospheric studies); the fourth coefficient $\dot{g}_2^0$ describes the northward shift of the axial dipole (Langel 1987).

This suggests (but does not prove) that diffusion-modified advection by the ocean flow is indeed the mechanism responsible for the observed secular variation of the Earth's main magnetic field.

Agreement is much worse for the next four coefficients. These coefficients are associated with the westward drift of the non-dipole field (Langel 1987). The westward drift (∼0.2° per year, or 0.5 mm s^{-1}) is observed in the North Atlantic and Europe—the area that also has the densest observatory coverage (Macmillan and Quinn 2000)—but is hardly noticeable in the rest of the world; in some areas eastward drift seems to occur (Langel 1987). Since the present calculation gives no preferential weighting to the North-Atlantic/Europe area, good agreement could hardly be expected for the coefficients associated with the westward drift. Nonetheless, the calculated values of $\dot{g}_2^1$, $\dot{g}_2^2$ and $\dot{h}_2^2$ are not far from their IGRF values in recent history (IGRF 2007, Langel 1987). For example, the IGRF 1985–1990 value for $\dot{g}_2^1$ is 3.0 nT yr^{-1}; the IGRF 2005 value for $\dot{h}_2^2$ is −14.0 nT yr^{-1}, etc.

8. Year-to-year changes in secular variation: analysis of data

The IGRF secular variation coefficients are, by definition, constant within each IGRF five-year interval, but the locally measured secular variation often changes substantially from year to year. (Local values of secular variation are the differences between successive annual means of the field components.) The mathematical approach described above, and used to obtain the results in table 1, is not suitable for predicting the local values of secular variation. By the very nature of the projection technique, its results, comprising the first few terms of the global spherical harmonic expansion, are not expected to approximate the local values well. Thus a completely different approach is needed; below, I present a comparison of previously published oceanographic and geomagnetic observational data. It demonstrates that the trend in secular variation is indeed closely correlated with the trend in the ocean-flow intensity.

The trend in secular variation, and, in particular, the abrupt changes in this trend—the geomagnetic jerks—are visible most clearly in the data from European observatories (De Michelis and Tozzi 2005). If secular variation owes its origin to the ocean flow, secular variation measured in Western Europe should be correlated with the intensity of the North Atlantic oceanic circulation. While correlation is expected, a direct proportionality is not: since the field satisfies $\nabla^2\mathbf{B} = 0$ at all times, secular variation in Europe, or at any other location, is influenced by the flow in all oceans (mathematically, through the action of the operator P_Y in equations (39)–(41)). Nevertheless, the influence of the nearest ocean should be particularly strong. This should be even more so for temporal variability, since major currents of different oceans are unlikely to vary synchronously. Both the pattern and the intensity of the North

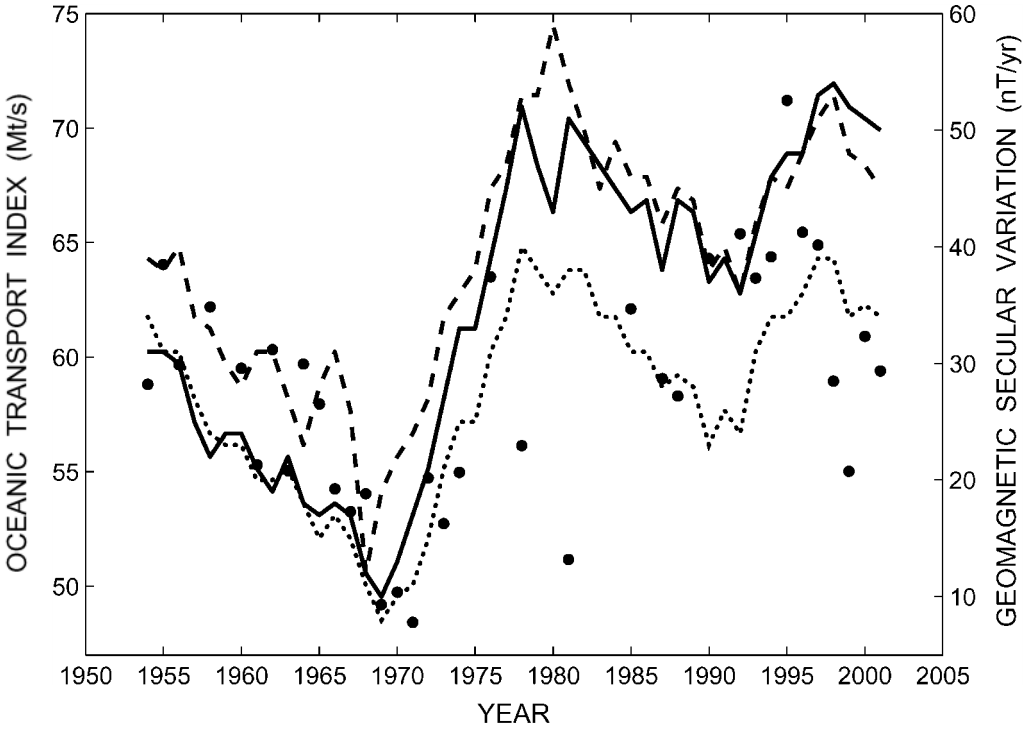

Figure 1. Does ocean flow cause the geomagnetic jerks? Comparison of oceanographic and geomagnetic data shows that the trend in secular variation is closely correlated with the trend in the ocean-flow intensity. Points—the oceanic transport index, a measure of intensity of the North Atlantic gyre circulation (Curry and McCartney 2001; data absent in some years, especially between 1979 and 1984). Lines—secular variation of the geomagnetic field (differences between successive annual means, east component) at three observatories in Western Europe: solid line—Eskdalemuir, dotted line—Niemegk, dashed line—Chambon la Foret (World Data Centre for Geomagnetism 2007). It is seen that the hitherto unexplained geomagnetic jerks of 1969, 1978, 1991 and 1998 (De Michelis and Tozzi 2005) are correlated with sharp changes in the trend of the ocean-flow intensity. See section 8 for details.

Atlantic circulation ought to exert strong influence on secular variation in Western Europe. However, the pattern does not vary with time as much as the intensity does, and its variability is not easily quantifiable. This leaves the intensity of the North Atlantic circulation as the best candidate for an attempt to discover temporal correlation with secular variation in Western Europe.

The intensity of the North Atlantic gyre circulation was recently quantified by oceanographers (Curry and McCartney 2001), the result being the transport index for the years 1954 to 2001. (Data absent in some years, especially between 1979 and 1984.) Figure 1 shows that this index and secular variation in Western Europe are indeed correlated. In particular, the hitherto unexplained geomagnetic jerks of 1969, 1978, 1991 and 1998 (De Michelis and Tozzi 2005) are correlated with sharp changes in the trend of the ocean-flow intensity.

Also explained thereby is the recently discovered (Gallet *et al* 2005) correlation between secular variation and the climate in Western Europe: the latter is strongly influenced by the

atmospheric North Atlantic Oscillation, which is the driving force behind the variability of the North Atlantic gyre circulation (Curry and McCartney 2001).

9. Some order-of-magnitude estimates and spatial correlations

The action of the operator P_Y in equation (41), which accounts for the effect of magnetic diffusion in the horizontal plane, precludes a point-by-point comparison between the local values of $-\mathbf{v}\cdot\nabla_h B_r$ and the locally measured values of $\partial B_r/\partial t$. Nevertheless, as a truncated Fourier-type expansion, P_Y is likely to preserve a signature of such well-localized features of $-\mathbf{v}\cdot\nabla_h B_r$ that stand out in magnitude (though the peak value is likely to be reduced). Thus, an attempt can be made to produce order-of-magnitude estimates of $-\mathbf{v}\cdot\nabla_h B_r$ in those locations of the world ocean where significant effects may be expected, and then compare these estimates with observations represented by the IGRF-based global distribution of $\partial B_r/\partial t$.

Since only a very rough agreement can be expected, I will consider only the dominant axial-dipole field. (This is not a good approximation in high latitudes, or in the South Atlantic and Indian oceans.) The downward vertical component $Z = -B_r$ of the axial-dipole field

$$Z_0 = -2g_1^0 \cos\theta \approx (6\times 10^4\,\mathrm{nT})\cos\theta \tag{42}$$

changes only along the meridian, increasing in the northward direction at the rate $\sim 10\,\mathrm{nT\,km^{-1}}$ (in low latitudes). Thus only the meridional component of the velocity $\mathbf{v}$ is important for this estimate. The ocean currents in low to moderate latitudes with significant, and well localized, meridional transport are the three western boundary currents: the Gulf Stream between the Florida Straits and Cape Hatteras (the Florida Current), the North Brazil Current (including the Guiana Current) and the Kuroshio between the Philippines and Japan. (Also the Agulhas, but in its vicinity the geomagnetic field is nowhere near the axial-dipole field.) For these currents, a rough order-of-magnitude estimate for $\mathbf{v}$ is $1\,\mathrm{mm\,s^{-1}} \approx 30\,\mathrm{km\,yr^{-1}}$; higher values occur locally within the currents, but for present purposes the average over the width $\sim 10^3$ km is appropriate. (With $N = 10$, the minimum half-wavelength in the spherical harmonic expansion is $\sim 2\times 10^3$ km.) A rough estimate of the magnitude of $-\mathbf{v}\cdot\nabla_h Z_0$ is then $300\,\mathrm{nT\,yr^{-1}}$. The sign of $-\mathbf{v}\cdot\nabla_h Z_0$ should be negative because meridional transport is northward in all three currents.

Remarkably, the world chart of $\partial Z/\partial t$ shows a pronounced local maximum (by absolute value) in the neighborhood of each of the three currents, see figure 2, reproduced from figure 42 of Langel (1987). Indeed, these three maxima stand out as the key features of the chart. One of these local maxima is also the global one, located east of Florida, with $\partial Z/\partial t \approx -180\,\mathrm{nT\,yr^{-1}}$. At the maximum east of North Brazil, $\partial Z/\partial t \approx -160\,\mathrm{nT\,yr^{-1}}$; at the maximum south of the Philippines, $\partial Z/\partial t \approx -80\,\mathrm{nT\,yr^{-1}}$. That is, not only the spatial correlation is strong, but the agreement with the above order-of-magnitude estimate is quite good as well. The charts for other IGRF five-year intervals will differ, of course, but the maxima persist. The two maxima in the central Atlantic have since moved closer to Florida and to North Brazil, while the maximum in the western Pacific is currently near Japan.

It is tempting to consider also the effect of the Antarctic Circumpolar Current, the strongest ocean current (cf Manoj *et al* 2006, Vivier *et al* 2004). However, an order-of-magnitude analysis similar to the above is not likely to succeed in this case, for several reasons. The meridional component of velocity in this current is weak, and the geomagnetic field cannot be approximated by the axial-dipole field. Most importantly, the current is not at all well localized. The contribution of the Antarctic Circumpolar Current to secular variation should be significant,

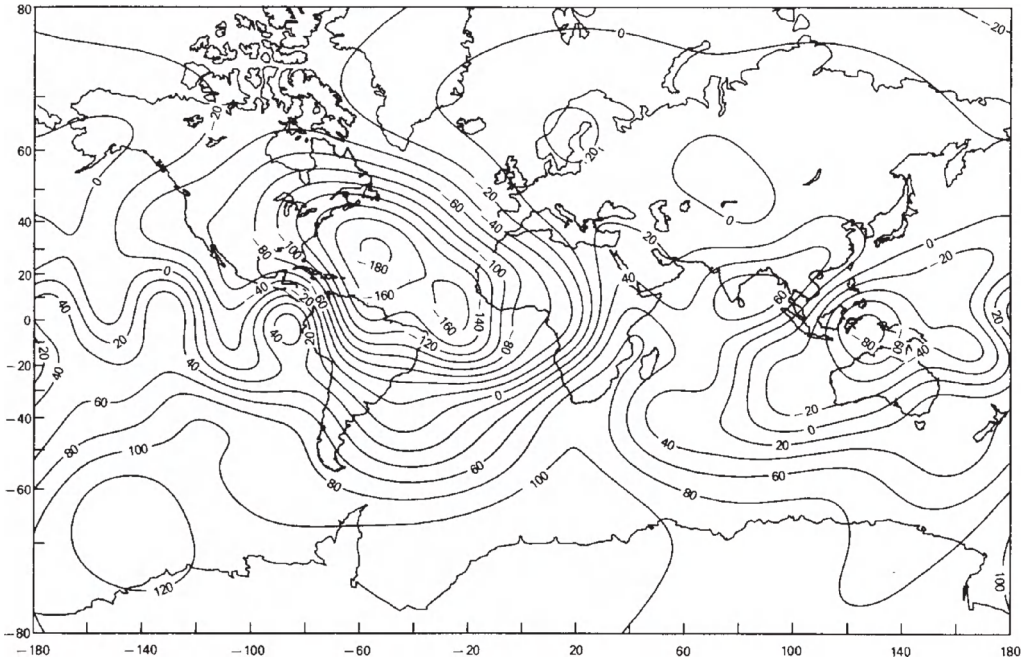

Figure 2. World chart of geomagnetic secular variation at 1980 (vertical component, $\partial Z/\partial t$) reproduced from figure 42 of Langel (1987). Units are $\mathrm{nT\,yr^{-1}}$; Mercator projection. Three local maxima (by absolute value) stand out as the key features of the chart; they are located east of Florida, east of North Brazil and south of the Philippines. Each of these maxima is associated with a major western boundary current: the Florida Current, the North Brazil Current and the Kuroshio, respectively. Not only the spatial correlation is strong, but also agreement is good between the local rates of secular variation and the order-of-magnitude estimates based on the currents' total transports. See section 9 for details.

and figure 2 does show large values of $\partial Z/\partial t$ throughout the region, but an easily recognizable spatial correlation, as in the cases discussed above, cannot be expected.

10. Why the Earth's magnetic moment changes slowly

The spherical harmonic coefficients of the observed secular variation do not exhibit any obvious pattern, with one exception: whereas the main field itself is strongly dominated by its axial-dipole part, the secular variation is not. As a result, the relative secular change of the axial-dipole part of the main field is much slower than that of some other main-field harmonics. This fact is important (the Earth's magnetic moment would have been changing much faster otherwise), and has been discussed for as long as secular variation has been represented in spherical harmonics, but no explanation of it exists.

If secular variation is caused by the ocean flow, a simple explanation of this fact can be given. Consider first some preliminary matters. Since the surface flow $\mathbf{v}(\theta, \phi, t)$ is non-divergent (equation (25)), the total flux of $\mathbf{v}$ across any closed curve drawn on the Earth's surface is zero.

In particular, this applies to every parallel, so the following is always true

$$\int_0^{2\pi} v_\theta \, \mathrm{d}\phi = 0, \tag{43}$$

where v_θ is the meridional component of $\mathbf{v}$.

Consider now the contribution to the right-hand side of equation (41) of the axial-dipole part of the main field (with the Gauss coefficient g_1^0). This contribution is proportional to $P_Y(v_\theta \sin\theta)$. Calculation of the spherical harmonic coefficients, implied by P_Y, entails multiplication of $v_\theta \sin\theta$ by $P_l^m(\cos\theta)\cos m\phi$ or $P_l^m(\cos\theta)\sin m\phi$ and integration over the unit sphere. In the cases where $m = 0$, the quantity $v_\theta \sin\theta P_l^0(\cos\theta)$ must be integrated. Because of equation (43), all such $m = 0$ integrals will vanish.

This means that the axial dipole that dominates the main field makes no contribution to the axial-dipole coefficient $\dot{g}_1^0$ of secular variation (or to any other $\dot{g}_l^0$). It is not surprising, then, that secular variation is not dominated by its axial-dipole part.

11. Conclusions

The results presented suggest that the observed secular variation of the Earth's magnetic field owes its origin to the ocean flow. A numerical simulation using the induction equation of magnetohydrodynamics and the ocean flow field yields secular variation in rough agreement with observations. Data analysis exhibits striking temporal correlation between the intensity of the North Atlantic oceanic circulation and secular variation in Western Europe; this explains, in particular, the geomagnetic jerks, and the recently discovered correlation between secular variation and climate. Spatial correlation between ocean currents and secular variation is also strong.

There is little doubt that these conclusions will be met with skepticism. And so they should: the results presented by no means constitute a proof. But the possibility of direct connection between the ocean flow and the secular variation of the geomagnetic field is bound to stimulate further research, especially in view of the implications for the question of the origin of the main field.

The current consensus is that the main field is generated by the hydromagnetic dynamo in the Earth's fluid outer core. Secular variation has been taken as evidence of motion in the core since the time of Halley (1692). Halley thought that secular variation, the westward drift in particular, was caused by differential rotation of a magnetized solid core, separated from the 'external parts of the Globe' (also magnetized) by a 'fluid medium'. Contemporary theoretical studies use the westward drift to estimate the characteristic large-scale velocity in the outer core, and to conclude that dynamo action is possible. If secular variation is caused by the ocean flow, the entire concept of the dynamo operating in the Earth's core is called into question: there exists no other evidence of hydrodynamic flow in the core.

Acknowledgments

The ocean state estimate was provided by the ECCO Consortium for Estimating the Circulation and Climate of the Ocean funded by the National Oceanographic Partnership Program (NOPP). The geomagnetic observatory data were provided by the World Data Centre for Geomagnetism

(Edinburgh) operated by the British Geological Survey. The spherical harmonics software was kindly provided by R L Parker. I thank A Bayliss, W R Burghardt, A B Kostinski and M Strelets for comments and criticism.

References

Backus G, Parker R and Constable C 1996 *Foundations of Geomagnetism* (Cambridge: Cambridge University Press)

Batchelor G K 1967 *An Introduction to Fluid Dynamics* (Cambridge: Cambridge University Press)

Bloxham J, Gubbins D and Jackson A 1989 Geomagnetic secular variation *Phil. Trans. R. Soc.* A **329** 415–502

Callarotti R C and Schmidt P E 1983 Inductive response of metallic spheres and spherical shells *J. Appl. Phys.* **54** 2940–6

Chorin A J 1969 On the convergence of discrete approximations to the Navier–Stokes equations *Math. Comput.* **23** 341–53

Curry R G and McCartney M S 2001 Ocean gyre circulation changes associated with the North Atlantic Oscillation *J. Phys. Oceanogr.* **31** 3374–400

De Michelis P and Tozzi R 2005 A local intermittency measure (LIM) approach to the detection of geomagnetic jerks *Earth Planet. Sci. Lett.* **235** 261–72

ECCO 2007 *Consortium for Estimating the Circulation and Climate of the Ocean* http://www.ecco-group.org

Gallet Y, Genevey A and Fluteau F 2005 Does Earth's magnetic field secular variation control centennial climate change? *Earth Planet. Sci. Lett.* **236** 339–47

Gorban A N and Karlin I V 2005 *Invariant Manifolds for Physical and Chemical Kinetics* (Berlin: Springer)

Halley E 1692 An account of the cause of the change of the variation of the magnetical needle; with an hypothesis of the structure of the internal parts of the Earth: as it was proposed to the Royal Society in one of their late meetings *Phil. Trans.* **16** 563–78

Halmos P R 1957 *Introduction to Hilbert Space and the Theory of Spectral Multiplicity* 2nd edn (New York: Chelsea)

Hulot G, Eymin C, Langlais B, Mandea M and Olsen N 2002 Small-scale structure of the geodynamo inferred from Oersted and Magsat satellite data *Nature* **416** 620–3

IGRF 2007 *International Geomagnetic Reference Field* http://www.ngdc.noaa.gov/IAGA/vmod/

Köhl A, Stammer D and Cornuelle B 2007 Interannual to decadal changes in the ECCO global synthesis *J. Phys. Oceanogr.* **37** 313–37

Kuvshinov A V 2008 3-D global induction in the oceans and solid earth: recent progress in modeling magnetic and electric fields from sources of magnetospheric, ionospheric and oceanic origin *Surv. Geophys.* **29** 139–86

Langel R A 1987 The main field *Geomagnetism* vol 1 ed J A Jacobs (London: Academic) pp 249–512

Macmillan S and Quinn J M 2000 The 2000 revision of the joint UK/US geomagnetic field models and an IGRF 2000 candidate model *Earth Planets Space* **52** 1149–62 http://www.terrapub.co.jp/journals/EPS/abstract/5212/52121149.html

Manoj C, Kuvshinov A, Maus S and Lühr H 2006 Ocean circulation generated magnetic signals *Earth Planets Space* **58** 429–37 http://www.terrapub.co.jp/journals/EPS/abstract/5804/58040429.html

Moffatt H K 1978 *Magnetic Field Generation in Electrically Conducting Fluids* (Cambridge: Cambridge University Press)

Olsen N and Mandea M 2008 Rapidly changing flows in the Earth's core *Nat. Geosci.* **1** 390–4

Olson P and Aurnou J 1999 A polar vortex in the Earth's core *Nature* **402** 170–3

Pedlosky J 1996 *Ocean Circulation Theory* (Berlin: Springer)

Press W H, Teukolsky S A, Vetterling W T and Flannery B P 1992 *Numerical Recipes in FORTRAN: The Art of Scientific Computing* 2nd edn (Cambridge: Cambridge University Press)

Schutz B 1980 *Geometrical Methods of Mathematical Physics* (Cambridge: Cambridge University Press)

Stephenson D and Bryan K 1992 Large-scale electric and magnetic fields generated by the oceans *J. Geophys. Res.* **97** 15467–80

Taylor G 1953 Dispersion of soluble matter in solvent flowing slowly through a tube *Proc. R. Soc.* A **219** 186–203

Tyler R H, Maus S and Lühr H 2003 Satellite observations of magnetic fields due to ocean tidal flow *Science* **299** 239–41

Tur A V and Yanovsky V V 1993 Invariants in dissipationless hydrodynamic media *J. Fluid Mech.* **248** 67–106

Vivier F, Maier-Reimer E and Tyler R H 2004 Simulations of magnetic fields generated by the Antarctic Circumpolar Current at satellite altitude: can geomagnetic measurements be used to monitor the flow? *Geophys. Res. Lett.* **31** L10306

World Data Centre for Geomagnetism (Edinburgh) 2007 Worldwide Observatory Annual Means http://www.geomag.bgs.ac.uk/gifs/annual_means.shtml

Wunsch C and Heimbach P 2007 Practical global oceanic state estimation *Physica* D **230** 197–208

Young W R and Jones S 1991 Shear dispersion. *Phys. Fluids* A **3** 1087–101